

# A Data Centric Approach for Unsupervised Domain Generalization via Retrieval from Web Scale Multimodal Data

Christopher Liao<sup>1</sup> Theodoros Tsiligkaridis<sup>2</sup> Brian Kulis<sup>1</sup>

## Abstract

Domain generalization (DG) is an important problem that learns a model that can generalize to unseen test domains leveraging one or more source domains, under the assumption of shared label spaces. However, most DG methods assume access to abundant source data in the target label space, a requirement that proves overly stringent for numerous real-world applications, where acquiring the same label space as the target task is prohibitively expensive. For this setting, we tackle the multimodal version of the *unsupervised domain generalization* (UDG) problem, which uses a large *task-agnostic unlabeled* source dataset, such as LAION-2B during finetuning. Our framework does not explicitly assume any relationship between the source dataset and target task. Instead, it relies only on the premise that the source dataset can be efficiently searched in a joint vision-language space. For this multimodal UDG setting, we propose a novel method to build a small (<100K) subset of the source data in three simple steps: (1) diversified retrieval using label names as queries, (2) rank pseudo-labeling, and (3) clustering to find representative samples. To demonstrate the value of studying the multimodal UDG problem, we compare our results against state-of-the-art source-free DG and zero-shot (ZS) methods on their respective benchmarks and show up to 10% improvement in accuracy on 20 diverse target datasets. Additionally, our multi-stage dataset construction method achieves 3% improvement on average over nearest neighbors retrieval. Code is available: <https://github.com/Chris210634/mudg>

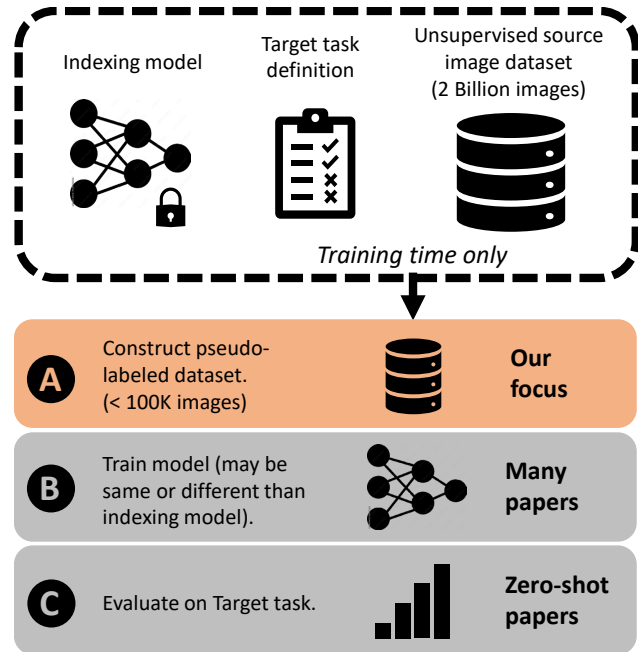


Figure 1. Proposed multimodal unsupervised domain generalization (MUDG) setup. For finetuning, we are given: a large indexed unlabeled source image dataset, the CLIP model used to search the index, and the target task definition (i.e. label names). We follow a 3-step experimental procedure: (A) construct a pseudo-labeled subset of the source data, (B) train the student CLIP model, and (C) evaluate on the target task. We focus on *step A* using a *small-scale* subset of source data.

## 1. Introduction

Domain generalization (DG) is widely studied in the computer vision literature because the train and test image data distributions are different for many applications. However, traditional DG methods assume access to labeled task-specific source data, which is expensive for many real-world applications. Consequently, more recent studies have tackled the unsupervised DG (UDG) problem, where source labels are not used during finetuning (Zhang et al., 2022; Narayanan et al., 2022; Harary et al., 2022). Unfortunately, this experimental procedure is fairly restrictive and impractical, since it still assumes that the source and target label spaces are identical. To address the shortcoming, we pro-

<sup>1</sup>Department of Electrical and Computer Engineering, Boston University <sup>2</sup>MIT Lincoln Laboratory. Correspondence to: Christopher Liao <cli25@bu.edu>, Theodoros Tsiligkaridis <ttsili@ll.mit.edu>, Brian Kulis <bkulis@bu.edu>.

pose to study a more realistic multimodal UDG (MUDG) setting, where the source data is both unlabeled and “task-agnostic”, i.e. we do not assume any relationship between the source and target label spaces. When the task-specific assumption is relaxed, large-scale source data can be leveraged, as it can be crawled cheaply from the web.

### Multimodal unsupervised domain generalization

**(MUDG)** In order to leverage publicly available unlabeled web-crawled image data, such as LAION (Schuhmann et al., 2022), we propose MUDG, a more general variation of the UDG classification problem. “Multimodal” refers to the requirement for the source dataset to be efficiently searchable in a joint vision-language space using a pretrained CLIP model. Using this searchable index, our goal is to build a pseudo-labeled subset of the source data to train a student CLIP model for a given target classification task. See Figure 1 and Table 1 for a concise illustration of our problem setting. In particular, our work can be viewed as an extension of the recent source free domain generalization (SFDG) problem (Cho et al., 2023), which only uses the target task definition during finetuning. Compared to SFDG, finding a suitable subset of the source data adds complexity to algorithm design, but our results show that the margin for accuracy improvement is much larger under our MUDG setting.

**Data-centric focus** As Figure 1 illustrates, we focus on developing a method to construct a pseudo-labeled subset of the source data for finetuning. For training, we use simple selective finetuning and prompt tuning, using the cross-entropy loss, as this is not the focus of our work. In contrast, a large body of work under the umbrella of “webly supervised” classification (Chen & Gupta, 2015; Li et al., 2020) focuses almost exclusively on developing training algorithms to learn from noisy web-crawled data, using the same fixed datasets collected from a search engine (Li et al., 2017b; Sun et al., 2021). We hope to complement webly supervised methods by redirecting some focus toward how the finetuning dataset can be built from large open-source datasets (Schuhmann et al., 2022). This “data-centric” perspective on method development is growing in popularity in the pretraining literature, especially with last year’s DataComp initiative (Gadre et al., 2023). However, most data-centric works currently focus on distilling datasets to build more robust foundational models at an industrial scale, whereas our paper focuses on task-specific finetuning using a much smaller subset of images.

**Method overview** Toward our central goal of developing a strong method for task-specific dataset construction, we propose a pipeline of three steps in Figures 2 and 3. (1) *Diversified retrieval*: augment the text prototypes using pseudo-random tokens according to waffleCLIP (Roth et al.,

Setting	Task-agnostic Source	Task-specific Source	Unlabeled Target	Task Definition
DA	-	labeled	✓	✓
SFDA	-	-	✓	✓
ZS	-	-	-	-
DG	-	labeled	-	✓
UDG	-	unlabeled	-	✓
SFDG	-	-	-	✓
<b>MUDG</b>	✓	-	-	✓

Table 1. Comparison of problem settings based on the information available at training time. DA - domain adaptation; DG - domain generalization; SF - source free; ZS - zero-shot. UDG - unsupervised DG. MUDG - multimodal UDG is our setting. Compared to SFDG, MUDG requires an additional large unlabeled dataset, which is not task-specific, such as LAION-2B.

2023), e.g. “a photo of a chicken, ⟨random⟩.” Retrieve the nearest neighbors of each augmented text prototype. The purpose of this step is to diversify the retrieved images; for example, a dataset with only one type of chicken is undesirable. (2) *Rank pseudo-labeling*: label each retrieved image with the closest text prototype in the CLIP embedding space. We use retrieval rank to determine the closeness of image and text feature pairs, as opposed to using the cosine similarity directly. This mitigates the well-known “hubness” effect in the retrieval literature (Radovanovic et al., 2010; Bogolin et al., 2022). (3) *Clustering*: cluster image embeddings into  $k$  clusters within each label group and randomly select one sample from each cluster. The purpose of this step is twofold: to build a balanced dataset, with  $k$  samples per label; and to assure that no two images are semantically similar. Section 3 explains the reasoning for each step in more detail. We use the same finetuning procedure for all experiments to focus our study on evaluating the proposed dataset building pipeline.

Our main contributions are:

1. We introduce the multimodal UDG problem, a more modern variation on the traditional UDG problem and a more tractable problem than source free DG.
2. We present an intuitive data-centric method for MUDG.
3. We present results on 20 diverse image classification datasets. We observe up to 10% improvements in target accuracy compared to the SFDG and ZS baselines. This shows that there is promise in studying the MUDG problem.
4. We compare our proposed dataset construction pipeline with baseline retrieval methods, achieving 3% improvement on average over nearest neighbor retrieval.

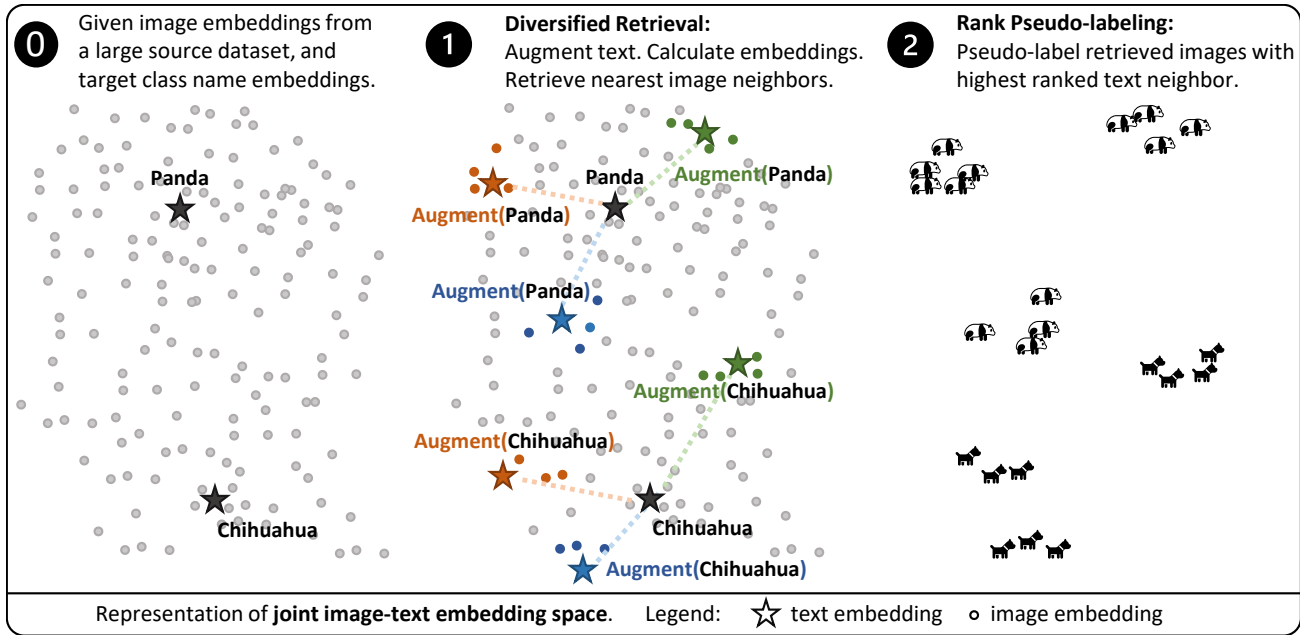


Figure 2. Illustration of our three step pipeline for constructing a finetuning dataset.

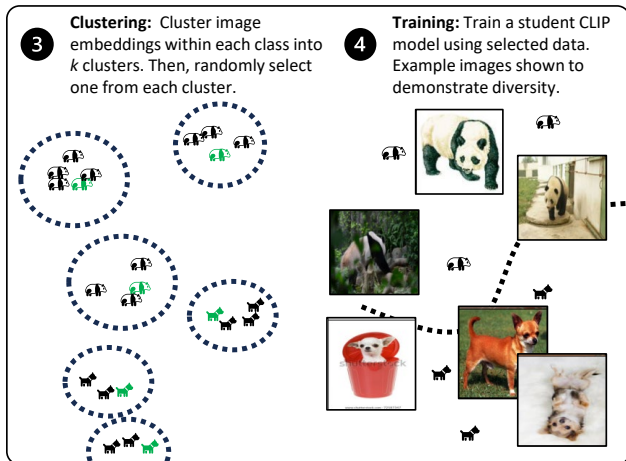


Figure 3. Continuation of Figure 2.

## 2. Related Works

**Multimodal foundational models** Multimodal foundational models such as CLIP (Radford et al., 2021), ALIGN (Jia et al., 2021), BLIP (Li et al., 2022b), and CoCa (Yu et al., 2022) use separate image and language encoders to embed the two modalities into a joint space. Once pretrained, these embeddings can be used to create an open-sourced database searchable by both image and text (Schuhmann et al., 2022). Efficient search on a scale of billions of images is enabled by approximate nearest neighbor search libraries such as FAISS (Douze et al., 2024). A recent work (Gadre et al., 2023) achieved the latest state-of-the-art on ZS ImageNet

by cleaning LAION-5B with a teacher CLIP model. Another recent work (Sun et al., 2023) uses a large CLIP model and unpaired web-crawled data to train a smaller foundational model in a distillation-inspired manner. The above works focus on generalist pretraining from scratch, which remains out-of-reach of most academic researchers. We focus instead on task-specific finetuning using a constructed dataset of up to 100K samples. Our work is most similar to React (Liu et al., 2023), which tackles the “model customization” problem. In comparison, our work is more focused on the source subset construction portion of the finetuning pipeline, and consequently, we achieve similar accuracy improvements as React with a 100× smaller retrieved dataset.

**Flavors of domain generalization** Table 1 is a non-exhaustive summary of variations on generalization settings studied in recent literature. Domain adaptation (Sun et al., 2016; Saito et al., 2019; Acuna et al., 2021) aims to leverage out-of-distribution (OOD) but task-specific source data in conjunction with unlabeled target data. Traditional DG (Muandet et al., 2013; Cha et al., 2022; Min et al., 2022) trains on OOD task-specific source data from multiple domains, without knowledge of target data. A more recent flavor of DG (Shu et al., 2023; Khattak et al., 2023) trains on generic labeled source data (e.g. ImageNet) with the goal of generalizing to any classification task, by leveraging transferability of the image-text alignment in CLIP. Unsupervised DG (Zhang et al., 2022; Narayanan et al., 2022; Harary et al., 2022) trains on unlabeled task-specific source data. Source-free DG (SFDG) (Cho et al., 2023) aims to

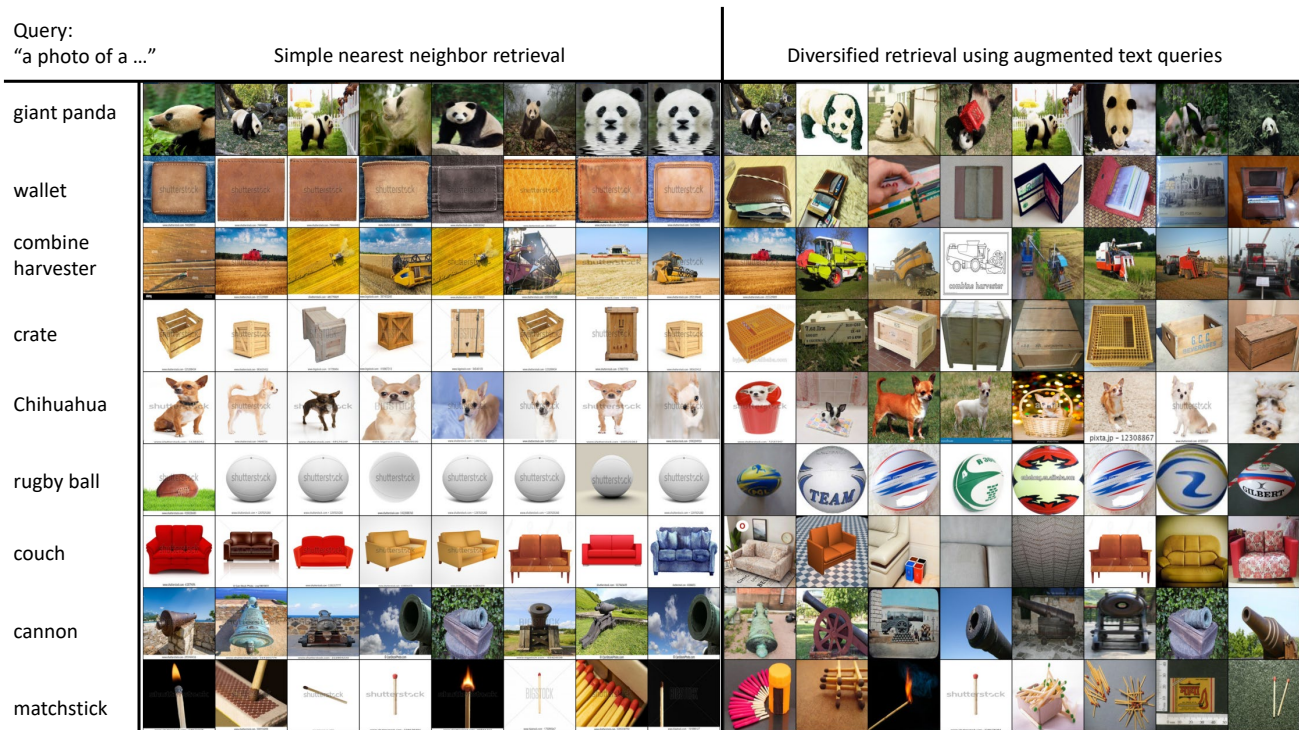


Figure 4. Qualitative results for step 1: diversified retrieval. Left: nearest neighbors to text query in LAION-2B. Right: images retrieved using diversified text features. Images retrieved using diverse queries cover a broader spectrum of appearances in the wild.

increase pretrained accuracy with only the target task information, but the improvement over ZS methods is not consistent empirically. ZS methods (Menon & Vondrick, 2022; Pratt et al., 2023; Roth et al., 2023) improve accuracy by ensembling multiple text features. Our problem setting, multimodal UDG, takes advantage of plentiful unlabeled non-task-specific image data, which offers more leverage than the SFDG setting, while not relying on any task-specific or labeled images contrary to the DA and DG studies.

**Webly supervised, open world, and open set** The webly supervised literature (Chen & Gupta, 2015; Li et al., 2020) focuses on learning from a noisy web-crawled dataset (Li et al., 2017b; Sun et al., 2021) and is very closely related to the large body of work on noisy supervised learning, see survey (Song et al., 2022). These works focus on the finetuning algorithm given a dataset, rather than the construction of the training data, unlike our work. Another popular research direction focuses on generalization to unseen classes given a certain set of (possibly related) training classes; these works fall under open-set (Saito et al., 2021; Du et al., 2023; Panareda Busto & Gall, 2017) open-world (Bendale & Boult, 2015; Boult et al., 2019; Cao et al., 2022) or base-to-novel (Zhou et al., 2022; Khattak et al., 2023; Kan et al., 2023) semi-supervised learning. Finally, some works selectively retrieve from an unlabeled data pool to

expand a smaller set of labeled training samples (Sener & Savarese, 2017; Killamsetty et al., 2021; Kim et al., 2023), referred to as core-set sampling. Contrary to these works, we assume no labeled data of any kind at training time. Retrieval augmentation (Blattmann et al., 2022; Gur et al., 2021; Long et al., 2022; Iscen et al., 2023) is a related line of work which requires a retrieval system at test time, adding substantially heavier evaluation overhead.

### 3. Method

Our main method consists of a three-stage pipeline presented in Figures 2 and 3 used to build a pseudo-labeled subset of the source data. We then use the standard cross entropy loss to finetune the last three layers of the student CLIP encoders along with the text prompt. This finetuning procedure is not the focus of our work, but details are included in the Experiments section.

**Assumptions and notation.** We are given an unlabeled source dataset  $\mathcal{X}_s$  (e.g. LAION-2B English, with text labels discarded).  $\mathcal{X}_s$  must be indexed in a joint image-text embedding space by a pair of CLIP encoders  $f_{\text{index, text}}$  and  $f_{\text{index, image}}$ . Both are frozen. We are also given label tokens for the target classification task, formatted as "a photo of a  $\langle \text{class name} \rangle$ ", and denoted as  $\{t_1, \dots, t_c\}$  where  $c$  is the number of classes. The goal is to optimize a "student" CLIP

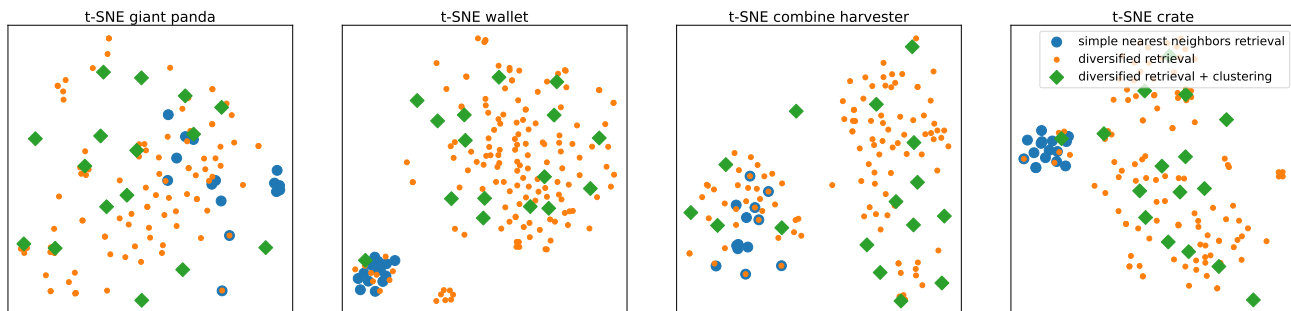


Figure 5. t-SNE plots of image features in the indexing model’s embedding space, showing the benefits of steps 1 and 3. Simple nearest neighbor retrieval (blue circle) covers only a small portion of the image distribution for each label. Diversified retrieval (orange dot) covers a broader portion of the image distribution, but contains semantically-redundant samples. After the clustering step (green diamond), the selected image samples are evenly spaced across the entire distribution, and thus the best representation for each label.

model  $f_{\text{student}}$  to classify images from the given classes. Note that  $f_{\text{student}}$  and  $f_{\text{index}}$  can be the same or different models, and we experiment with both possibilities.

### 3.1. Step 1: Diversified Retrieval

*Goal:* Retrieve a diverse set of image data for training.

The simplest way to build a dataset from the list of class names is to calculate the text feature for each class and retrieve the nearest neighbors from  $\mathcal{X}_s$ . This is straightforward, but the results are not promising as shown in the left of Figure 4. The retrieved images are not identical, but contain very little variation. For instance, images of wallets only contain one possible orientation; images of couches only contain stock photos of a perfect couch. Figure 6 (the line with blue x) shows that when trained on these images, the model severely overfits to the retrieved dataset. To diversify the dataset, we augment the query text tokens using WaffleCLIP (Roth et al., 2023), which appends random characters to the end of the query, conceptually similar to adding random tokens. Concretely, let  $\{\mathcal{A}_1, \dots, \mathcal{A}_m\}$  denote a set of  $m$  text augmentation functions. We construct a dataset with  $mc$  queries:  $\{f_{\text{index}, \text{text}}(\mathcal{A}_j(\mathbf{t}_i)) \mid \forall i = 1 : c, j = 1 : m\}$ . We retrieve the  $n$  nearest neighbors to each query in  $\mathcal{X}_s$  and remove redundancies, resulting in a preliminary dataset size of at most  $mcn$ .

For choosing the augmentation function, we consider two factors: (1) the augmented query text does not change the label of the original text; and (2) the resulting distribution of augmented queries covers the entire concept of the class. Intuitively, WaffleCLIP is likely to preserve the label of the original text, since it only appends random tokens to the end of the class name. From inspecting Figure 4 right, WaffleCLIP also seems to capture a broad range of visual variation within each class. We also demonstrate this diversity using t-SNE plots in Figure 5.

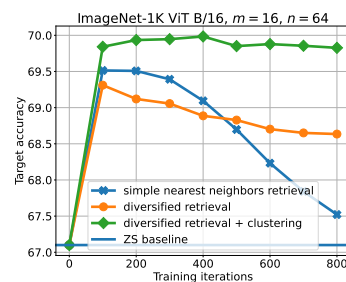


Figure 6. Target accuracy vs. training iterations for the datasets corresponding to Figure 5 (colors match). This confirms our intuition that both the diversified retrieval and clustering steps are necessary.

### 3.2. Step 2: Rank Pseudo-labeling

*Goal:* Mitigate hubness effect.

This step is a small digression from the main story, please skip to step 3 for high-level understanding. If each image sample is only retrieved by queries from one label, then pseudo-labeling is trivial. However, there is a large amount of overlap between retrievals from different labels, especially for datasets with a large number of classes or fine-grained concepts. For each image that is retrieved by multiple queries, we can assign it either (1) the label of the closest text feature as measured by their cosine similarity, or (2) the label of the text feature to which it is ranked the highest. We choose the latter option (detailed concretely in Algorithm 1) to address the well-known hubness effect (Radovanovic et al., 2010). In simple terms, hubs are samples in the dataset which tend to be closer to other samples in a high-dimensional embedding space, regardless of relevance. Specific to our application, a “hub” text feature is one that is close to a disproportionately large number of image samples, resulting in a large number of image samples being assigned the hub label. In other words, the pseudo-label is biased towards any hubs in the label space when cosine similarity is used directly. However, when we use rank to assign labels, the hub label cannot be overused because closeness to the hub is determined by rank relative to other image samples.

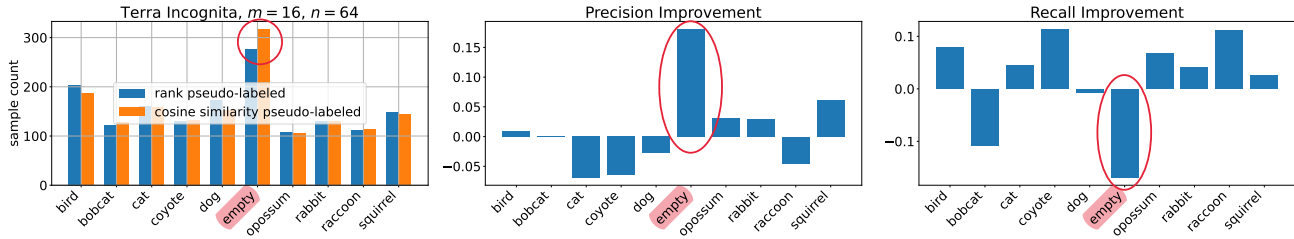


Figure 7. Hubness effect and the value of pseudo-labeling based on rank (step 2). The x-axis labels are the label names for Terra Incognita. The label “empty” is a hub because about 50 more images were labeled as empty when cosine similarity is used instead of rank (left bar plot). The right two bar plots show the precision and recall improvement of rank labeling over cosine similarity labeling, after clustering and training. Rank labeling improves precision for images labeled as empty while improving the recall for most animal images. This is desirable: The cost of mislabeling an animal image as empty is much greater than the cost of mislabeling an empty image.

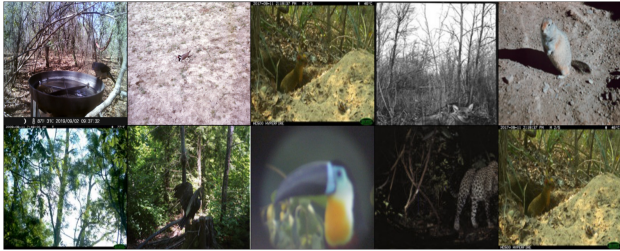


Figure 8. A selection of images from the 50 that were labeled as “empty” by cosine similarity but as one of the animals by rank.

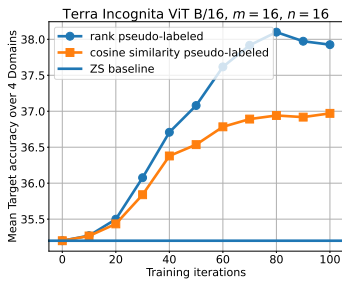


Figure 9. Target accuracy vs. training iterations for the two datasets constructed for Figure 7 left. Colors match. This confirms our intuition that rank labeling improves overall target accuracy in addition to the good precision-recall properties in Figure 7 right.

Not all datasets have hubs, but we found that the Terra Incognita dataset illustrates the effect perfectly. This dataset contains camera trap images of different animals, and the labels are the animal names along with “empty” for empty images. As a case study, we retrieve images from LAION-2B using step 1 and the query: “a photo of a (class name), from a camera trap.”. We then compare pseudo-labeling using cosine similarity versus using rank. The left bar plot in Figure 7 shows that cosine similarity pseudo-labeling assigns some images the “empty” label, which are labeled as one of the animals when using rank. Figure 8 displays examples of these images. For this dataset, “empty” likely functions as a hub, since many camera-trap images are mostly empty, especially if the animal is small. We verify in the two right bar plots of Figure 7 that using rank pseudo-labeling improves the recall of most animal images at the expense of

**Algorithm 1** MUDG

**Input:** Source dataset  $\mathcal{X}_s$ , searchable in logarithmic time with indexing model  $f_{\text{index, image}}$ ,  $m$  augmentation functions  $\mathcal{A}_1 \dots \mathcal{A}_m$ ,  $n, k$ , pretrained  $f_{\text{index}}$  and  $f_{\text{student}}$ , class name tokens  $\{t_1, \dots, t_c\}$ .

**Step 1:** Let  $\mathcal{Q} = \{f_{\text{index, text}}(\mathcal{A}_j(t_i)) \mid \forall i = 1 : c, j = 1 : m\}$  denote the query set. For each  $q \in \mathcal{Q}$ , retrieve  $n$  nearest neighbors in  $\mathcal{X}_s$ . Combine retrieved samples from all queries and denote as  $\mathcal{X}_1$ .

**Step 2:** For each query  $q \in \mathcal{Q}$ , sort image samples  $\mathbf{x} \in \mathcal{X}_1$  by decreasing cosine similarity between  $q$  and  $f_{\text{index, image}}(\mathbf{x})$ . Denote the rank of  $\mathbf{x}$  relative to  $q$  as  $\text{rank}(\mathbf{x}, q) \geq 1$ . Then, assign each  $\mathbf{x} \in \mathcal{X}_1$  the label corresponding to the closest query in terms of rank, i.e.  $\arg \min_q \text{rank}(\mathbf{x}, q)$ . Denote the labeled set as  $\mathcal{X}_2$ .

**Step 3:** Initialize an empty labeled dataset  $\mathcal{X}_3$ . For each label  $y \in 1 : c$ : Find the subset of  $\mathcal{X}_2$  with label  $y$ . Calculate their embeddings with  $f_{\text{index, image}}$ . Cluster into  $k$  clusters, using k-means. Randomly select one sample from each cluster and append to  $\mathcal{X}_3$ .  $\mathcal{X}_3$  contains  $ck$  samples.

**Step 4:** Finetune  $f_{\text{student}}$  on  $\mathcal{X}_3$  for  $N$  iterations, using standard cross entropy loss.

**Output:** finetuned  $f_{\text{student}}$

decreasing the recall of empty images. This is a favorable trade-off for this application. We further verify in Figure 9 that rank pseudo-labeling improves the overall accuracy as well, compared to cosine similarity labeling.

**3.3. Step 3: Clustering**

*Goal:* Select representative samples and balance the label distribution.

Referring back to Figure 6, note that the dataset resulting from diversified retrieval (in orange) actually lowers target accuracy on ImageNet when used to train the student CLIP model, despite containing a large number of samples

## A Data Centric Baseline for Unsupervised Domain Generalization

	Setting	ImageNet	Caltech	Pets	Cars	Flowers	Food	Aircraft	SUN	DTD	EuroSAT	UCF	Mean
<b>Open-AI CLIP ViT-B/16</b>													
CLIP ZS (Radford et al., 2021)	ZS	67.1	93.3	89.0	65.4	71.0	85.7	24.9	63.2	43.6	46.6	67.4	65.2
waffleCLIP (Roth et al., 2023)	ZS	68.2	93.5	88.1	65.5	72.1	85.9	25.6	66.2	44.3	47.3	68.1	65.9
Random Descriptors (Roth et al., 2023)	ZS	68.1	94.3	87.7	65.7	71.7	85.7	25.2	66.2	44.7	47.7	67.3	65.8
Handcrafted Ensemble (Radford et al., 2021)	ZS	68.4	93.5	88.8	66.0	71.1	86.0	24.9	66.0	43.9	45.0	68.0	65.6
GPT Descriptors (Menon & Vondrick, 2022)	ZS	68.6	93.7	89.0	65.1	72.1	85.7	23.9	67.4	43.9	46.4	66.8	65.7
Nearest neighbors	MUDG	69.4	93.9	<b>93.4</b>	70.2	75.8	86.3	27.2	67.4	52.4	41.2	69.9	67.9
Skip clustering step	MUDG	69.1	<b>94.4</b>	93.1	73.0	76.4	86.2	<b>33.7</b>	68.4	54.0	57.9	71.8	70.7
<b>MUDG (ours)</b>	MUDG	<b>69.9</b>	94.1	<b>93.4</b>	<b>73.7</b>	<b>76.8</b>	<b>86.6</b>	<b>33.7</b>	<b>68.8</b>	<b>54.1</b>	<b>58.5</b>	<b>72.8</b>	<b>71.1</b>
gain over ZS		+2.8	+0.8	+4.5	+8.3	+5.8	+0.9	+8.8	+5.6	+10.6	+11.9	+5.4	+5.9
gain over waffleCLIP		+1.7	+0.7	+5.4	+8.1	+4.7	+0.7	+8.0	+2.6	+9.8	+11.1	+4.6	+5.2
<b>Open-AI CLIP ViT-L/14</b>													
CLIP ZS (Radford et al., 2021)	ZS	73.8	94.6	93.6	76.9	79.4	90.9	32.8	68.0	52.7	56.2	74.7	72.1
waffleCLIP (Roth et al., 2023)	ZS	75.0	96.1	93.5	77.1	78.8	90.9	33.6	69.3	54.3	57.7	75.3	72.9
Random Descriptors (Roth et al., 2023)	ZS	75.1	<b>96.9</b>	93.4	76.7	78.5	90.7	33.6	70.1	54.5	59.3	75.5	73.1
Handcrafted Ensemble (Radford et al., 2021)	ZS	75.6	95.6	94.0	78.1	79.8	91.2	32.7	70.5	54.0	55.2	75.0	72.9
GPT Descriptors (Menon & Vondrick, 2022)	ZS	75.3	96.7	93.8	77.4	79.3	90.9	34.8	71.0	56.4	62.8	73.9	73.8
Nearest neighbors	MUDG	76.2	95.8	95.3	78.0	<b>80.2</b>	<b>91.3</b>	33.3	71.7	56.2	61.6	75.6	74.1
Skip clustering step	MUDG	75.5	96.0	95.3	79.3	79.7	91.2	<b>36.6</b>	72.2	56.3	<b>69.5</b>	<b>76.5</b>	75.3
<b>MUDG (ours)</b>	MUDG	<b>76.3</b>	95.9	<b>95.5</b>	<b>79.9</b>	<b>80.2</b>	<b>91.3</b>	<b>36.6</b>	<b>72.8</b>	<b>57.2</b>	67.9	<b>76.5</b>	<b>75.5</b>
gain over ZS		+2.5	+1.3	+1.9	+3.0	+0.8	+0.5	+3.8	+4.8	+4.5	+11.7	+1.8	+3.3
gain over waffleCLIP		+1.3	-0.1	+1.9	+2.8	+1.4	+0.4	+3.0	+3.5	+3.0	+10.2	+1.2	+2.6

Table 2. Comparison of our MUDG baseline with ZS baselines on 11 diverse datasets. Average of three experiments. For MUDG rows, dataset construction and model training is separate for each dataset. “Nearest neighbors” refers to simple nearest neighbors retrieval; “Skip clustering step” refers to omitting step 3 in our pipeline.

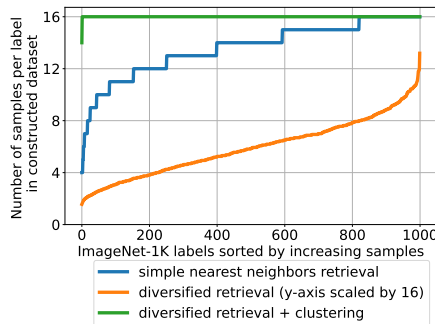


Figure 10. Label distribution of datasets constructed before and after clustering (step 3). For this figure,  $m = n = k = 16$ .

( $\mathcal{O}(mcn)$ ). This stems from two problems: (1) Some images are semantic-duplicates as evident by the small clusters of orange dots in Figure 5, e.g. pictures of the same object in different orientations. (2) The dataset is imbalanced as shown by the orange distribution over labels in Figure 10. This is simply caused by asymmetries in the retrieval and download process (e.g. dead links, linked image changed since dataset creation, etc.). As a result, the training process overfits to dominant semantic-duplicate images and the pseudo-label distribution; both are artifacts of the dataset construction process.

To address both of the above issues, we first use k-means clustering to cluster the image features in the embedding space of the indexing model into  $k \ll mcn$  clusters, then randomly select an image from each cluster. If  $k$  is chosen conservatively, semantic duplicates fall into a single cluster, and only one can be selected for the final training set. Additionally, each label should have  $k$  training samples. Figure 10 illustrates the final balanced label distribution in

green, and Figure 6 shows the corresponding target accuracy improvements in matching colors. For reference, ImageNet-1K has  $c = 1000$  labels, and we found  $m = 16$ ,  $n = 64$  and  $k = 48$  to yield good results.

## 4. Experiments

We experiment with the ViT B/16 and ViT L/14 pretrained weights released by Radford et al. (2021) and available through the Python openclip package (Ilharco et al., 2021). The indexing model is ViT L/14; we use an index released by the LAION team built using the FAISS package (Douze et al., 2024). For details, please see the GitHub repository. The source dataset is LAION-2B-en (Schuhmann et al., 2022). We experiment with two model sizes to show that we achieve large gains in target accuracies even when the indexing model and the student model are identical.

**Datasets** We experiment with a diverse set of target classification tasks. ImageNet-1K (Russakovsky et al., 2015), Caltech-101 (Li et al., 2022a), Oxford-Pets (Parkhi et al., 2012), Stanford-Cars (Krause et al., 2013), Flowers-102 (Nilsback & Zisserman, 2008), Food-101 (Bossard et al., 2014), FGVC-Aircraft (Maji et al., 2013), SUN-397 (Xiao et al., 2010), Describable-Textures (DTD) (Cimpoi et al., 2013), EuroSAT (Helber et al., 2019), UCF-101 (an action recognition dataset) (Soomro et al., 2012) in Table 2 and ImageNet-V2 (Recht et al., 2019), ImageNet-Sketch (Wang et al., 2019), ImageNet-A (natural adversarial examples) (Hendrycks et al., 2021b), and ImageNet-R (Hendrycks et al., 2021a) in Table 3 are commonly used by zero-shot papers, while Office Home (Venkateswara et al., 2017),

## A Data Centric Baseline for Unsupervised Domain Generalization

		ImageNet					Office Home					Terra Incognita				
		V2	Sketch	A	R	Mean	A	C	P	R	Mean	100	38	43	46	Mean
<b>Open-AI CLIP ViT-B/16</b>																
CLIP ZS	ZS	60.9	46.6	47.2	74.1	57.2	82.6	67.2	88.8	89.6	82.1	51.5	26.1	34.1	29.3	35.2
waffleCLIP	ZS	61.8	48.5	50.0	76.3	59.2	83.1	68.2	89.7	90.4	82.9	54.2	29.5	36.4	<b>30.6</b>	<b>37.7</b>
Random Descriptors	ZS	61.7	48.8	49.9	76.6	59.2	83.0	69.1	89.5	90.2	83.0	51.3	21.7	36.7	28.8	34.6
Handcrafted Ensemble	ZS	61.9	48.5	49.2	77.9	59.4	84.3	67.7	89.3	90.2	82.9	<b>55.4</b>	28.5	33.4	31.0	37.1
GPT Descriptors	ZS	61.8	48.1	48.6	75.2	58.4	-	-	-	-	-	-	-	-	-	-
PromptStyler †	SFDG	-	-	-	-	-	83.8	68.2	91.6	90.7	83.6	-	-	-	-	-
<b>MUDG (ours)</b>	<b>MUDG</b>	<b>63.0</b>	<b>49.9</b>	<b>50.6</b>	<b>78.6</b>	<b>60.5</b>	<b>85.4</b>	<b>72.8</b>	<b>91.9</b>	<b>91.3</b>	<b>85.4</b>	53.3	<b>32.3</b>	<b>37.7</b>	25.3	37.2
gain over ZS		+2.1	+3.4	+3.4	+4.5	+3.3	+2.8	+5.6	+3.2	+1.8	+3.3	+1.8	+6.2	+3.6	-4.0	+1.9
gain over waffle		+1.2	+1.4	+0.6	+2.3	+1.4	+2.2	+4.6	+2.3	+0.9	+2.5	-0.9	+2.9	+1.3	-5.3	-0.5
<b>Open-AI CLIP ViT-L/14</b>																
CLIP ZS	ZS	68.0	57.9	68.3	85.5	69.9	87.1	74.8	93.1	93.4	87.1	46.3	50.9	43.0	32.4	43.1
waffleCLIP	ZS	68.8	58.7	70.1	87.1	71.2	87.7	78.2	93.8	94.4	88.5	45.6	45.2	43.7	31.4	41.4
Random Descriptors	ZS	69.2	59.1	70.5	87.1	71.5	88.2	78.4	94.4	94.0	88.7	40.9	36.3	38.5	26.3	35.5
Handcrafted Ensemble	ZS	69.9	59.7	70.2	87.8	71.9	88.5	76.9	93.8	94.5	88.4	47.5	50.9	41.8	30.5	42.7
GPT Descriptors	ZS	69.4	58.8	69.6	86.4	71.1	-	-	-	-	-	-	-	-	-	-
PromptStyler †	SFDG	-	-	-	-	-	89.1	77.6	<b>94.8</b>	<b>94.8</b>	89.1	-	-	-	-	-
<b>MUDG (ours)</b>	<b>MUDG</b>	<b>70.4</b>	<b>60.6</b>	<b>71.5</b>	<b>88.7</b>	<b>72.8</b>	<b>90.3</b>	<b>80.9</b>	<b>94.8</b>	<b>94.8</b>	<b>90.2</b>	<b>49.3</b>	<b>54.4</b>	<b>44.6</b>	<b>32.5</b>	<b>45.2</b>
gain over ZS		+2.4	+2.7	+3.2	+3.2	+2.9	+3.2	+6.2	+1.7	+1.4	+3.1	+3.0	+3.5	+1.6	+0.1	+2.1
gain over waffle		+1.6	+1.9	+1.4	+1.6	+1.6	+2.6	+2.8	+1.1	+0.5	+1.7	+3.7	+9.3	+0.9	+1.1	+3.8

Table 3. Comparison of our MUDG baseline with ZS baselines and PromptStyler on DG benchmarks. Average of three trials. Dataset construction and model training is performed once and evaluated on all domains for Office Home, Terra Incognita, and DomainNet; but we perform the steps separately for each ImageNet domain, due to differences in label spaces. PromptStyler (Cho et al., 2023) † results are those reported by the authors; all other results are our reproductions.

		DomainNet						
		C	I	P	Q	R	S	Mean
<b>Open-AI CLIP ViT-B/16</b>								
CLIP ZS		71.4	47.1	66.2	13.8	83.4	63.4	57.6
waffleCLIP		73.0	52.0	68.3	14.0	84.9	65.8	59.7
Random Desc.		73.5	51.0	67.6	14.6	84.7	65.9	59.6
Ensemble		73.7	51.2	<b>69.3</b>	<b>16.0</b>	85.0	<b>66.2</b>	60.2
PromptStyler †		73.1	50.9	68.2	13.3	<b>85.4</b>	65.3	59.4
<b>MUDG (ours)</b>		<b>74.6</b>	<b>53.6</b>	68.9	15.4	85.2	66.1	<b>60.6</b>
gain over ZS		+3.2	+6.5	+2.7	+1.6	+1.8	+2.6	+3.1
gain over waffle		+1.5	+1.7	+0.6	+1.4	+0.3	+0.3	+1.0
<b>Open-AI CLIP ViT-L/14</b>								
CLIP ZS		79.5	52.2	70.9	22.5	86.8	71.5	63.9
waffleCLIP		80.4	56.5	72.8	22.0	88.1	73.0	65.4
Random Desc.		80.6	56.0	73.4	23.3	87.9	73.2	65.7
Ensemble		81.1	55.8	73.9	<b>24.2</b>	87.9	73.7	66.1
PromptStyler †		80.7	55.6	73.8	21.7	88.2	73.2	65.5
<b>MUDG (ours)</b>		<b>81.5</b>	<b>58.6</b>	<b>74.4</b>	23.1	<b>88.4</b>	<b>74.0</b>	<b>66.7</b>
gain over ZS		+2.0	+6.4	+3.5	+0.6	+1.6	+2.5	+2.8
gain over waffle		+1.1	+2.1	+1.6	+1.1	+0.4	+1.0	+1.2

Table 4. DomainNet Results, continued from Table 3.

Terra Incognita (Beery et al., 2018), DomainNet (Peng et al., 2019), VLCS (Torralba & Efros, 2011), and PACS (Li et al., 2017a) are common DG and DA datasets. VLCS and PACS results are in Appendix A, since they are less challenging.

**Baselines** We compare to both ZS and SFDG baselines, since they achieve similar results on average, despite SFDG having stronger assumptions. Note that all ZS and SFDG baselines (other than CLIP ZS) ensemble multiple text features at test time; MUDG baselines do not require ensembling at test time, and this is a slight advantage. The published ZS baseline methods are: waffleCLIP (Roth et al., 2023), handcrafted ensemble (Radford et al., 2021) and GPT descriptors (Menon & Vondrick, 2022). We also include

a strong random descriptor baseline which ensembles randomly selected GPT descriptors, introduced by waffleCLIP. Note that the handcrafted ensemble is manually engineered for standard visual domains (e.g. painting and sketch), so achieves the highest accuracy on some DomainNet subsets, but under-performs significantly on fine-grained tasks. To the best of our knowledge, PromptStyler (Cho et al., 2023) is the only current SFDG baseline.

**Ablations** We provide two ablation comparisons across 11 datasets in Table 2 in the MUDG setting. We first show that our retrieval pipeline improves average accuracy by 3.2% over nearest neighbors retrieval for the B/16 model size. We then show that omitting the clustering step decreases average accuracy by 0.4%. Also importantly, the clustering step decreases the training dataset size significantly.

**Hyperparameters** See Tables 6 and 7 of the Appendix. An ablation study on  $m$ ,  $n$ , and  $k$  is included in Figure 11.

## 5. Conclusion

This work introduced the multimodal unsupervised domain generalization problem, an extension of the zero-shot and source-free domain generalization problems. MUDG uses a searchable, large, non-task-specific, unlabeled dataset, which adds substantial leverage over existing variations of the DG/ZS problem. We proposed an intuitive three-stage process for creating a task-specific subset of the source data, and reported promising accuracy improvements across 20 diverse benchmarks. This work highlights the importance of the dataset construction step of the finetuning pipeline, and further complements existing work on finetuning methods.



## Impact Statement

This paper presents work whose goal is to advance the field of Machine Learning. There are many potential societal consequences of our work, none which we feel must be specifically highlighted here.

## Acknowledgments

DISTRIBUTION STATEMENT A. Approved for public release. Distribution is unlimited.

This material is based upon work supported by the Under Secretary of Defense for Research and Engineering under Air Force Contract No. FA8702-15-D-0001. Any opinions, findings, conclusions or recommendations expressed in this material are those of the author(s) and do not necessarily reflect the views of the Under Secretary of Defense for Research and Engineering.

## References

- Acuna, D., Zhang, G., Law, M. T., and Fidler, S. f-domain adversarial learning: Theory and algorithms. In *International Conference on Machine Learning*, pp. 66–75. PMLR, 2021.
- Beery, S., Van Horn, G., and Perona, P. Recognition in terra incognita. In *Proceedings of the European conference on computer vision (ECCV)*, pp. 456–473, 2018.
- Bendale, A. and Boulton, T. Towards open world recognition. In *Proceedings of the IEEE conference on computer vision and pattern recognition*, pp. 1893–1902, 2015.
- Blattmann, A., Rombach, R., Oktay, K., Müller, J., and Ommer, B. Retrieval-augmented diffusion models. *Advances in Neural Information Processing Systems*, 35: 15309–15324, 2022.
- Bogolin, S.-V., Croitoru, I., Jin, H., Liu, Y., and Albanie, S. Cross modal retrieval with querybank normalisation. In *Proceedings of the IEEE/CVF Conference on Computer Vision and Pattern Recognition*, pp. 5194–5205, 2022.
- Bossard, L., Guillaumin, M., and Van Gool, L. Food-101 – mining discriminative components with random forests. In *European Conference on Computer Vision*, 2014.
- Boulton, T. E., Cruz, S., Dhamija, A. R., Gunther, M., Henrydoss, J., and Scheirer, W. J. Learning and the unknown: Surveying steps toward open world recognition. In *Proceedings of the AAAI conference on artificial intelligence*, volume 33, pp. 9801–9807, 2019.
- Cao, K., Brbic, M., and Leskovec, J. Open-world semi-supervised learning. In *International Conference on Learning Representations (ICLR)*, 2022.
- Cha, J., Lee, K., Park, S., and Chun, S. Domain generalization by mutual-information regularization with pre-trained models. In *European Conference on Computer Vision*, pp. 440–457. Springer, 2022.
- Chen, X. and Gupta, A. Webly supervised learning of convolutional networks. In *Proceedings of the IEEE international conference on computer vision*, pp. 1431–1439, 2015.
- Cho, J., Nam, G., Kim, S., Yang, H., and Kwak, S. Prompt-styler: Prompt-driven style generation for source-free domain generalization. In *Proceedings of the IEEE/CVF International Conference on Computer Vision*, pp. 15702–15712, 2023.
- Cimpoi, M., Maji, S., Kokkinos, I., Mohamed, S., and Vedaldi, A. Describing textures in the wild. *CoRR*, abs/1311.3618, 2013. URL <http://arxiv.org/abs/1311.3618>.
- Douze, M., Guzhva, A., Deng, C., Johnson, J., Szilvasy, G., Mazaré, P.-E., Lomeli, M., Hosseini, L., and Jégou, H. The faiss library. *arXiv preprint arXiv:2401.08281*, 2024.
- Du, P., Zhao, S., Sheng, Z., Li, C., and Chen, H. Semi-supervised learning via weight-aware distillation under class distribution mismatch. In *Proceedings of the IEEE/CVF International Conference on Computer Vision*, pp. 16410–16420, 2023.
- Gadre, S. Y., Ilharco, G., Fang, A., Hayase, J., Smyrnis, G., Nguyen, T., Marten, R., Wortsman, M., Ghosh, D., Zhang, J., et al. Datacomp: In search of the next generation of multimodal datasets. *arXiv preprint arXiv:2304.14108*, 2023.
- Gur, S., Neverova, N., Stauffer, C., Lim, S.-N., Kiela, D., and Reiter, A. Cross-modal retrieval augmentation for multi-modal classification. In *Findings of the Association for Computational Linguistics: EMNLP 2021*, pp. 111–123, 2021.
- Harary, S., Schwartz, E., Arbelle, A., Staar, P., Abu-Hussein, S., Amrani, E., Herzig, R., Alfassy, A., Giryas, R., Kuehne, H., et al. Unsupervised domain generalization by learning a bridge across domains. In *Proceedings of the IEEE/CVF Conference on Computer Vision and Pattern Recognition*, pp. 5280–5290, 2022.
- Helber, P., Bischke, B., Dengel, A., and Borth, D. Eurosat: A novel dataset and deep learning benchmark for land use and land cover classification. *IEEE Journal of Selected Topics in Applied Earth Observations and Remote Sensing*, 12(7):2217–2226, 2019.

- Hendrycks, D., Basart, S., Mu, N., Kadavath, S., Wang, F., Dorundo, E., Desai, R., Zhu, T., Parajuli, S., Guo, M., et al. The many faces of robustness: A critical analysis of out-of-distribution generalization. In *Proceedings of the IEEE/CVF International Conference on Computer Vision*, pp. 8340–8349, 2021a.
- Hendrycks, D., Zhao, K., Basart, S., Steinhardt, J., and Song, D. Natural adversarial examples. In *Proceedings of the IEEE/CVF Conference on Computer Vision and Pattern Recognition*, pp. 15262–15271, 2021b.
- Ilharco, G., Wortsman, M., Wightman, R., Gordon, C., Carlini, N., Taori, R., Dave, A., Shankar, V., Namkoong, H., Miller, J., Hajishirzi, H., Farhadi, A., and Schmidt, L. Openclip, July 2021. URL <https://doi.org/10.5281/zenodo.5143773>. If you use this software, please cite it as below.
- Iscen, A., Caron, M., Fathi, A., and Schmid, C. Retrieval-enhanced contrastive vision-text models. *arXiv preprint arXiv:2306.07196*, 2023.
- Jia, C., Yang, Y., Xia, Y., Chen, Y.-T., Parekh, Z., Pham, H., Le, Q., Sung, Y.-H., Li, Z., and Duerig, T. Scaling up visual and vision-language representation learning with noisy text supervision. In *International conference on machine learning*, pp. 4904–4916. PMLR, 2021.
- Kan, B., Wang, T., Lu, W., Zhen, X., Guan, W., and Zheng, F. Knowledge-aware prompt tuning for generalizable vision-language models. In *Proceedings of the IEEE/CVF International Conference on Computer Vision*, pp. 15670–15680, 2023.
- Khattak, M. U., Rasheed, H., Maaz, M., Khan, S., and Khan, F. S. Maple: Multi-modal prompt learning. In *Proceedings of the IEEE/CVF Conference on Computer Vision and Pattern Recognition*, pp. 19113–19122, 2023.
- Killamsetty, K., Zhao, X., Chen, F., and Iyer, R. Retrieve: Coreset selection for efficient and robust semi-supervised learning. *Advances in Neural Information Processing Systems*, 34:14488–14501, 2021.
- Kim, S., Bae, S., and Yun, S.-Y. Coreset sampling from open-set for fine-grained self-supervised learning. In *Proceedings of the IEEE/CVF Conference on Computer Vision and Pattern Recognition*, pp. 7537–7547, 2023.
- Krause, J., Stark, M., Deng, J., and Fei-Fei, L. 3d object representations for fine-grained categorization. In *Proceedings of the IEEE international conference on computer vision workshops*, pp. 554–561, 2013.
- Li, D., Yang, Y., Song, Y.-Z., and Hospedales, T. M. Deeper, broader and artier domain generalization. In *Proceedings of the IEEE international conference on computer vision*, pp. 5542–5550, 2017a.
- Li, F.-F., Andreeto, M., Ranzato, M., and Perona, P. Caltech 101, Apr 2022a.
- Li, J., Xiong, C., and Hoi, S. C. Mopro: Webly supervised learning with momentum prototypes. *arXiv preprint arXiv:2009.07995*, 2020.
- Li, J., Li, D., Xiong, C., and Hoi, S. Blip: Bootstrapping language-image pre-training for unified vision-language understanding and generation. In *International Conference on Machine Learning*, pp. 12888–12900. PMLR, 2022b.
- Li, W., Wang, L., Li, W., Agustsson, E., and Van Gool, L. Webvision database: Visual learning and understanding from web data. *arXiv preprint arXiv:1708.02862*, 2017b.
- Liu, H., Son, K., Yang, J., Liu, C., Gao, J., Lee, Y. J., and Li, C. Learning customized visual models with retrieval-augmented knowledge. In *Proceedings of the IEEE/CVF Conference on Computer Vision and Pattern Recognition*, pp. 15148–15158, 2023.
- Long, A., Yin, W., Ajanthan, T., Nguyen, V., Purkait, P., Garg, R., Blair, A., Shen, C., and van den Hengel, A. Retrieval augmented classification for long-tail visual recognition. In *Proceedings of the IEEE/CVF Conference on Computer Vision and Pattern Recognition*, pp. 6959–6969, 2022.
- Maji, S., Rahtu, E., Kannala, J., Blaschko, M. B., and Vedaldi, A. Fine-grained visual classification of aircraft. *CoRR*, abs/1306.5151, 2013. URL <http://arxiv.org/abs/1306.5151>.
- Menon, S. and Vondrick, C. Visual classification via description from large language models. *arXiv preprint arXiv:2210.07183*, 2022.
- Min, S., Park, N., Kim, S., Park, S., and Kim, J. Grounding visual representations with texts for domain generalization. In *European Conference on Computer Vision*, pp. 37–53. Springer, 2022.
- Muandet, K., Balduzzi, D., and Schölkopf, B. Domain generalization via invariant feature representation. In *International conference on machine learning*, pp. 10–18. PMLR, 2013.
- Narayanan, V., Deshmukh, A. A., Dogan, U., and Balasubramanian, V. N. On challenges in unsupervised domain generalization. In *NeurIPS 2021 Workshop on Pre-registration in Machine Learning*, pp. 42–58. PMLR, 2022.
- Nilsback, M.-E. and Zisserman, A. Automated flower classification over a large number of classes. In *2008*

- Sixth Indian Conference on Computer Vision, Graphics and Image Processing*, pp. 722–729, 2008. doi: 10.1109/ICVGIP.2008.47.
- Panareda Busto, P. and Gall, J. Open set domain adaptation. In *Proceedings of the IEEE international conference on computer vision*, pp. 754–763, 2017.
- Parkhi, O. M., Vedaldi, A., Zisserman, A., and Jawahar, C. Cats and dogs. In *2012 IEEE conference on computer vision and pattern recognition*, pp. 3498–3505. IEEE, 2012.
- Peng, X., Bai, Q., Xia, X., Huang, Z., Saenko, K., and Wang, B. Moment matching for multi-source domain adaptation. In *Proceedings of the IEEE International Conference on Computer Vision*, pp. 1406–1415, 2019.
- Pratt, S., Covert, I., Liu, R., and Farhadi, A. What does a platypus look like? generating customized prompts for zero-shot image classification. In *Proceedings of the IEEE/CVF International Conference on Computer Vision*, pp. 15691–15701, 2023.
- Radford, A., Kim, J. W., Hallacy, C., Ramesh, A., Goh, G., Agarwal, S., Sastry, G., Askell, A., Mishkin, P., Clark, J., Krueger, G., and Sutskever, I. Learning transferable visual models from natural language supervision, 2021.
- Radovanovic, M., Nanopoulos, A., and Ivanovic, M. Hubs in space: Popular nearest neighbors in high-dimensional data. *Journal of Machine Learning Research*, 11(sept): 2487–2531, 2010.
- Recht, B., Roelofs, R., Schmidt, L., and Shankar, V. Do imagenet classifiers generalize to imagenet? *CoRR*, abs/1902.10811, 2019. URL <http://arxiv.org/abs/1902.10811>.
- Roth, K., Kim, J. M., Koepke, A., Vinyals, O., Schmid, C., and Akata, Z. Waffling around for performance: Visual classification with random words and broad concepts. *arXiv preprint arXiv:2306.07282*, 2023.
- Russakovsky, O., Deng, J., Su, H., Krause, J., Satheesh, S., Ma, S., Huang, Z., Karpathy, A., Khosla, A., Bernstein, M., Berg, A. C., and Fei-Fei, L. ImageNet Large Scale Visual Recognition Challenge. *International Journal of Computer Vision (IJCV)*, 115(3):211–252, 2015. doi: 10.1007/s11263-015-0816-y.
- Saito, K., Kim, D., Sclaroff, S., Darrell, T., and Saenko, K. Semi-supervised domain adaptation via minimax entropy. In *Proceedings of the IEEE/CVF international conference on computer vision*, pp. 8050–8058, 2019.
- Saito, K., Kim, D., and Saenko, K. Openmatch: Open-set consistency regularization for semi-supervised learning with outliers. *arXiv preprint arXiv:2105.14148*, 2021.
- Schuhmann, C., Beaumont, R., Vencu, R., Gordon, C., Wightman, R., Cherti, M., Coombes, T., Katta, A., Mullis, C., Wortsman, M., et al. Laion-5b: An open large-scale dataset for training next generation image-text models. *Advances in Neural Information Processing Systems*, 35: 25278–25294, 2022.
- Sener, O. and Savarese, S. Active learning for convolutional neural networks: A core-set approach. *arXiv preprint arXiv:1708.00489*, 2017.
- Shu, Y., Guo, X., Wu, J., Wang, X., Wang, J., and Long, M. Clipood: Generalizing clip to out-of-distributions, 2023.
- Song, H., Kim, M., Park, D., Shin, Y., and Lee, J.-G. Learning from noisy labels with deep neural networks: A survey. *IEEE Transactions on Neural Networks and Learning Systems*, 2022.
- Soomro, K., Zamir, A. R., and Shah, M. UCF101: A dataset of 101 human actions classes from videos in the wild. *CoRR*, abs/1212.0402, 2012. URL <http://arxiv.org/abs/1212.0402>.
- Sun, B., Feng, J., and Saenko, K. Return of frustratingly easy domain adaptation. In *Proceedings of the AAAI conference on artificial intelligence*, volume 30, 2016.
- Sun, X., Zhang, P., Zhang, P., Shah, H., Saenko, K., and Xia, X. Dime-fm: Distilling multimodal and efficient foundation models. *arXiv preprint arXiv:2303.18232*, 2023.
- Sun, Z., Yao, Y., Wei, X.-S., Zhang, Y., Shen, F., Wu, J., Zhang, J., and Shen, H. T. Webly supervised fine-grained recognition: Benchmark datasets and an approach. In *Proceedings of the IEEE/CVF international conference on computer vision*, pp. 10602–10611, 2021.
- Torralba, A. and Efros, A. A. Unbiased look at dataset bias. In *CVPR 2011*, pp. 1521–1528. IEEE, 2011.
- Venkateswara, H., Eusebio, J., Chakraborty, S., and Panchanathan, S. Deep hashing network for unsupervised domain adaptation. In *Proceedings of the IEEE Conference on Computer Vision and Pattern Recognition*, pp. 5018–5027, 2017.
- Wang, H., Ge, S., Xing, E. P., and Lipton, Z. C. Learning robust global representations by penalizing local predictive power. *CoRR*, abs/1905.13549, 2019. URL <http://arxiv.org/abs/1905.13549>.
- Xiao, J., Hays, J., Ehinger, K. A., Oliva, A., and Torralba, A. Sun database: Large-scale scene recognition from abbey to zoo. In *2010 IEEE Computer Society Conference on Computer Vision and Pattern Recognition*, pp. 3485–3492, 2010. doi: 10.1109/CVPR.2010.5539970.

Yu, J., Wang, Z., Vasudevan, V., Yeung, L., Seyedhosseini, M., and Wu, Y. Coca: Contrastive captioners are image-text foundation models, 2022.

Zhang, X., Zhou, L., Xu, R., Cui, P., Shen, Z., and Liu, H. Towards unsupervised domain generalization. In *Proceedings of the IEEE/CVF Conference on Computer Vision and Pattern Recognition*, pp. 4910–4920, 2022.

Zhou, K., Yang, J., Loy, C. C., and Liu, Z. Learning to prompt for vision-language models. *International Journal of Computer Vision*, 130(9):2337–2348, jul 2022. doi: 10.1007/s11263-022-01653-1. URL <https://doi.org/10.1007/s11263-022-01653-1>.

## A Data Centric Baseline for Unsupervised Domain Generalization

	PACS					VLCS				
	A	C	P	S	Mean	Caltech	Labelme	SUN	VOC	Mean
<b>Open-AI CLIP ViT-B/16</b>										
CLIP ZS	97.1	99.0	99.9	88.0	96.0	99.9	68.3	75.3	85.5	82.2
waffleCLIP	97.3	99.0	99.9	90.3	96.6	99.9	68.6	74.4	86.3	82.3
Random Descriptors	97.1	<b>99.2</b>	99.9	89.2	96.4	99.9	70.3	77.9	<b>87.0</b>	<b>83.8</b>
Ensemble	97.6	<b>99.2</b>	99.9	89.9	96.7	99.9	<b>69.1</b>	76.4	84.2	82.4
PromptStyler †	97.6	99.1	99.9	<b>92.3</b>	<b>97.2</b>	99.9	71.5	73.9	86.3	82.9
<b>MUDG (ours)</b>	<b>97.9</b>	<b>99.2</b>	99.9	90.7	96.9	99.9	65.5	<b>78.5</b>	86.3	82.6
<b>Open-AI CLIP ViT-L/14</b>										
CLIP ZS	98.8	99.6	99.9	95.6	98.5	99.9	70.7	73.8	85.7	82.5
waffleCLIP	<b>99.1</b>	99.7	100.0	95.7	98.6	99.9	70.8	74.1	<b>87.1</b>	<b>83.0</b>
Random Descriptors	98.9	99.6	100.0	95.6	98.5	99.9	67.6	<b>78.0</b>	86.4	<b>83.0</b>
Ensemble	98.8	99.6	100.0	95.7	98.5	99.9	65.5	76.1	85.1	81.7
PromptStyler †	<b>99.1</b>	99.7	100.0	95.5	98.6	99.9	<b>71.1</b>	71.8	86.8	82.4
<b>MUDG (ours)</b>	98.8	99.6	100.0	95.8	98.6	99.9	70.0	75.5	86.0	82.9

Table 5. Comparison of our MUDG method with ZS baselines and PromptStyler on PACS and VLCS. Average of three trials. Dataset construction and model training is performed once and evaluated on all domains. † denotes author reported numbers; all other results are our reproductions.

### Limitations

Even though we do not explicitly assume any relationships between the source and target data, our work may not be applicable to problems where the target visual concepts are either not present in the source dataset or completely misaligned with corresponding language concepts. Possible examples include synthetic aperture radar images, images of tissue samples, or medical scans. Additionally, our method may not improve results on datasets where the zero-shot accuracy is already saturated. For example, the VLCS dataset contains 5 classes: bird, car, chair, dog, and person. Our method does not achieve any meaningful improvement over the ZS baseline on these simple classification tasks.

### A. Experimental Details and Additional Results

**Domain abbreviations** Office Home domains: A - art; C - clipart; P - product; R - real. Terra Incognita domain names are anonymous location identifiers for camera traps. DomainNet domains: C - clipart; I - infograph; P - painting; Q - quickdraw; R - real; S - sketch. PACS domains: A - art; C - cartoon; P - photo; S - sketch. VLCS domain names are dataset names.

**Hyperparameters** The finetuning parameters are displayed in Table 6. The training set construction parameters  $n$ ,  $m$ , and  $k$  are dataset-specific and listed in Table 7. Moreover, the number of training iterations  $N$  and query/prompt template also varies with the dataset, as listed in Table 7.

**Ablation study** An ablation study on the training set construction parameters  $n$ ,  $m$ , and  $k$  are included in Figure 11. We perform these experiments for ImageNet, DomainNet, and Office Home. When varying the values of  $n$  and  $m$ , we scale the value of  $k$  by the same amount. Note that changing the values of these hyperparameters changes the size of the training dataset. For example, scaling  $k$  by 2 scales the number of training samples by the same amount. The main take-away from Figure 11 is that increasing the number of samples in the training data improves the target accuracy, but only up to a point. The target accuracy saturates at some point, and it is not beneficial to increase  $n$ ,  $m$ , or  $k$  further.

**Additional Notes** We do not verify the check-sums of the downloaded images, instead we filter out retrieved images where the cosine similarity between the image embedding and query text embedding is very low ( $<0.25$ ). The size of the retrieved datasets is listed in Table 7, and we emphasize again that our framework achieves impressive improvements in accuracy with a small number of retrieved image samples ( $<100K$ ).

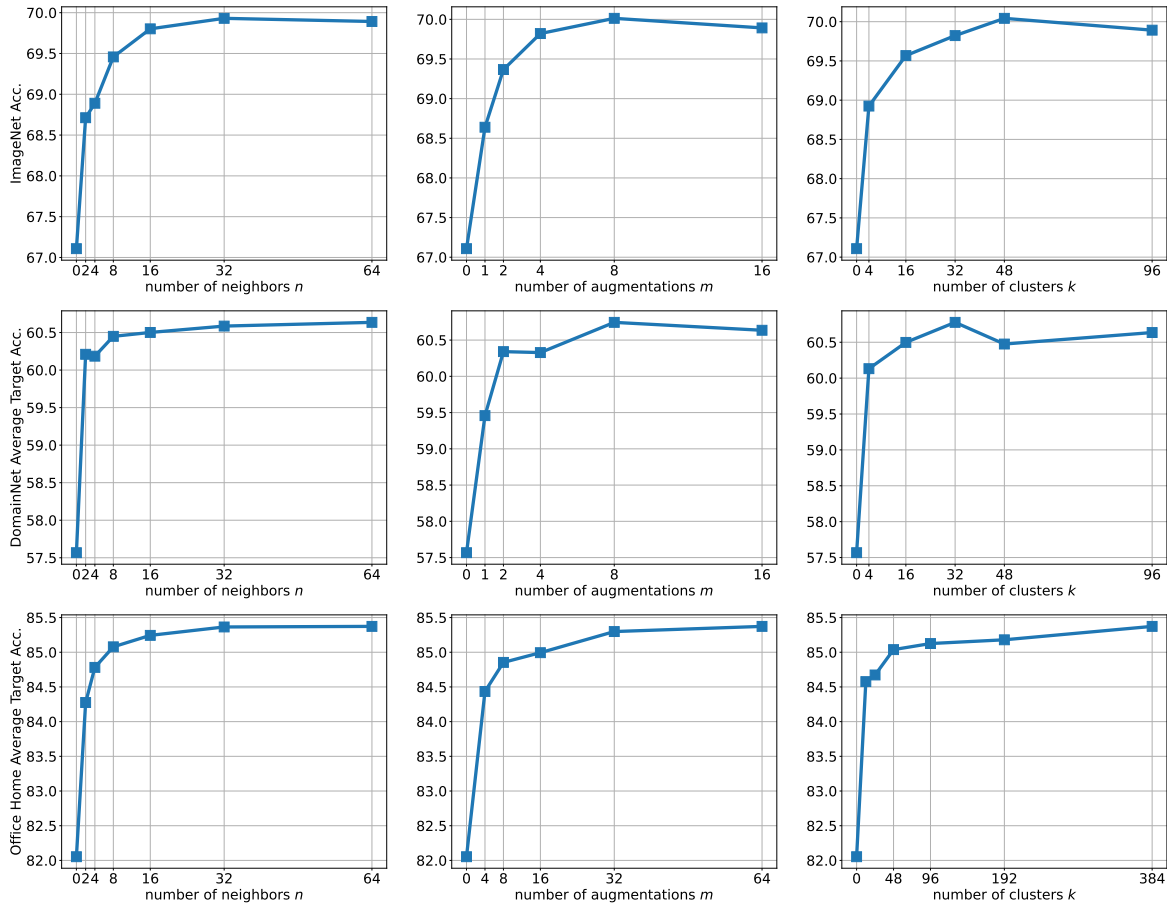


Figure 11. Ablation experiments for varying values of  $n$ ,  $m$  and  $k$ . Reference Algorithm 1 in the main paper and Table 7 in the Appendix for default values. Top row: ImageNet; middle row: DomainNet; bottom row: Office Home. Increasing either  $n$ ,  $m$  or  $k$  improves the target accuracy by retrieving a larger training set, but these plots show that the accuracy saturates at a certain value.

Finetuning Parameters		
	ViT-B/16	ViT-L/14
Finetune last 3 layers of text and vision encoders		
batch size	128	64
learning rate	0.00064	0.00016
weight decay	1e-5	
number of iterations ( $N$ )	dataset dependent	
learning rate decay	none	
softmax temperature	25	
optimizer	SGD momentum=0.9	
label smoothing	0	
EMA weight averaging $\beta$	0.995	
text prompt length	3	
text prompt initialization	“a photo of”	
text prompt learning rate multiplier	10 $\times$	
Parameters for Baselines		
WaffleCLIP ensemble size	8	

Table 6. Training hyperparameters.

Dataset	$n$	$m$	$k$	$N$	Actual training dataset size	Query template
ImageNet	64	16	96	300	96K	a photo of a {}.
Caltech	64	64	384	100	38K	a photo of a {}.
Pets	64	64	384	200	12K	a photo of a {}, a type of pet.
Cars	64	16	96	1000	18K	a photo of a {}.
Flowers	64	64	384	200	31K	a photo of a {}, a type of flower.
Food	64	64	384	100	34K	a photo of a {}, a type of food.
Aircraft	64	64	384	1000	26K	a photo of a {}, a type of aircraft.
SUN	64	16	96	300	38K	a photo of a {}.
DTD	64	64	384	200	18K	a photo of a {} texture.
EuroSAT	64	64	384	200	3K	a photo of a {}, from a satellite.
UCF	64	64	384	200	37K	a photo of a person doing {}.
ImageNet-V2	64	16	96	200	96K	a photo of a {}.
ImageNet-Sketch	64	16	96	200	96K	a photo of a {}.
ImageNet-A	64	16	96	200	19K	a photo of a {}.
ImageNet-R	64	16	96	200	19K	a photo of a {}.
DomainNet	64	16	96	200	33K	a photo of a {}.
Office Home	64	64	384	200	25K	a photo of a {}.
PACS	64	64	384	100	3K	a photo of a {}.
VLCS	64	64	384	50	2K	a photo of a {}.
Terra Incognita	64	64	384	100	3K	a photo of a {}, from a camera trap.

Table 7. Dataset-specific hyperparameters, reference Algorithm 1 in the main paper.  $n$  is number of nearest neighbors to be retrieved;  $m$  is number of text augmentations;  $k$  is number of k-means clusters;  $N$  is number of training iterations.